Bulgarian Chemical Communications, Volume 50, Special issue H (pp. 49–55) 2018

Modification and characterization of iron-containing biogenic materials as catalysts for the reaction of CO oxidation

T. M. Petrova*, D. G. Paneva, S. Zh. Todorova, Z. P. Cherkezova-Zheleva, D. G. Filkova, M. G. Shopska, N. I. Velinov, B. N. Kunev, G. B. Kadinov, I. G. Mitov

Institute of Catalysis, Bulgarian Academy of Sciences, Acad. G. Bonchev St., Bldg. 11, 1113 Sofia, Bulgaria

Received: February 12, 2018; Revised: March 14, 2018

The present study is focused on the preparation of modified iron-containing biogenic materials and testing them as catalysts for the reaction of CO oxidation. Modification was performed by impregnation of biogenic material obtained in Lieske cultivation medium. Impregnation was done using solutions of palladium chloride, cobalt nitrate, and manganese nitrate. Samples were characterized by X-ray diffraction, infrared spectroscopy, and Mössbauer spectroscopy. XRD results revealed that the starting biogenic material was X-ray amorphous, however, the presence of mixtures of low-crystalline iron oxyhydroxides, goethite and lepidocrocite, could not be excluded. Heating of Pd- and Co-modified materials led to the formation of oxide phases of Co_3O_4, γ-Fe_2O_3, and α-Fe_2O_3. Infrared spectra confirmed metal oxyhydroxide complete transformation to metal oxides in thermally treated samples. Mössbauer spectra of samples preheated at 300 °C indicated that the formed materials had a low degree of crystallinity, which is a specific feature of highly dispersed oxide materials. Doublet components in the Mössbauer spectra are indicative of nanosized highly dispersed particles demonstrating superparamagnetic behaviour. A ferrite $MnFe_2O_4$ phase was formed during synthesis of Mn-modified sample. Mössbauer spectra recorded at the temperature of liquid nitrogen showed a decrease of doublet part, which is typical of iron oxide particles of sizes below 4–10 nm. All the prepared samples were active in the reaction of CO oxidation, most active being manganese-modified catalyst. A synergistic effect was proposed between iron and manganese oxide components. Sample analysis after catalytic tests by means of Mössbauer spectroscopy revealed no changes in phase composition and dispersion.

Key words: biogenic iron-containing materials, chemical modification, X-ray diffraction, Infrared spectroscopy, Mössbauer spectroscopy, CO oxidation.

INTRODUCTION

Biogenic iron-containing materials are products of iron-transforming bacteria lifecycle [1–3]. Iron-containing bacteria of the *Sphaerotilus-Leptothrix* group are typical water representatives. In presence of these bacteria, Fe^{2+} ions are transformed into Fe^{3+} containing compounds [2,4–6]. These compounds are insoluble and the iron is deposited in the form of oxides, hydroxides, and salts [2,7–10], which have different phase composition, and different shape and size (globules, tubes, etc.). These materials demonstrate high specific surface area and high reactivity, which facilitate adsorption and decomposition of various contaminants [7–9,11–18]. Specific physical, chemical, and biological features of nanomaterials have motivated researchers for intensive studies. Iron oxides/hydroxides are a particular class of biocompatible compounds having natural biogenic analogues. Such materials being developed by various methods of synthesis are widely applied as catalysts. Many synthetic techniques for the production of various types of iron oxide nanoparticle materials (hematite, magnetite, goethite, etc.) are well established. However, most of these methods are costly and involve the use of hazardous chemicals [19]. Therefore, there is growing necessity to develop ecological and sustainable methods, such as biosynthesis [20]. Various studies have found that biogenic iron oxides, especially those of bacterial origin, are low crystalline aggregates composed of smaller species [7–10,17,21–23]. Biogenic iron specific properties are crucial for its application as an active component in catalysis in gaseous and liquid media [13,19,23–31], catalyst precursors [19,32], and catalysts [33]. In the course of the catalytic process, the stability of the biogenic materials is a very important property. In previous studies, it was found that their catalytic activity was preserved or slightly decreased after repeated use [26,32–35]. Actually, chemical modification of the biogenic materials is focused on improving some chemical properties.

This work is aimed at modifying iron containing biogenic materials by Pd, Co, and Mn and studying their catalytic behaviour in the reaction of CO oxidation.

* To whom all correspondence should be sent
E-mail: silberbarren@abv.bg

EXPERIMENTAL

Synthesis

Pd, Co, or Mn were deposited separately or in combination (Pd+Co) on biogenic iron-containing material by impregnation with solutions of $PdCl_2$, $Co(NO_3)_2.6H_2O$, and $Mn(NO_3)_2.4H_2O$, respectively. Basic biogenic material (BM) was prepared by *Leptothrix* genus bacteria cultivation in Lieske medium, which contained 0.3% Pd/Al-Si-O fibrous material. Proper concentrations of the selected salts were used so that chemical modifier content was 1 mass% Pd, 20 mass% Co, and 20 mass% Mn. Selected salts were dissolved in distilled water at room temperature under constant stirring. Three drops of 1N hydrochloric acid were added to the $PdCl_2$ solution to complete dissolution. Evaporation of the water was carried out at 60 °C and continuous stirring. The samples were further heated at the same temperature for 24 hours for complete drying. The same technique was applied for Co deposition on a sample containing 1% Pd. The samples are denoted as Pd/BM, Pd+Co/BM, Co/BM, and Mn/BM.

Before catalytic tests, the samples were calcined in air at 300 °C for 2 hours at a heating rate of 10 deg/min.

Characterization

Powder X-ray diffraction (XRD) patterns were collected by a TUR M62 diffractometer with Co Kα radiation. Phase identification was performed using ICDD-PDF2 database. Experimental XRD profiles of the studied ferrites were processed by using PowderCell-2.4 software and appropriate corrections for instrumental broadening.

Infrared (IR) spectra of the samples were recorded on a Nicolet 6700 FTIR spectrometer (Thermo Electron Corporation, USA) using the method of dilution in KBr pellets (0.5% of studied substance). The spectra were collected in the middle IR region using 100 scans at a resolution of 4 (data spacing 1.928 cm^{-1}).

Mössbauer spectra (MS) were registered in air at room temperature (RT) by means of Wissel (Wissenschaftliche Elektronik GmbH, Germany) electromechanical spectrometer working in a constant acceleration mode. A $^{57}Co/Rh$ (activity ≅ 20 mCi) source and α-Fe standard were used. Experimentally obtained spectra were fitted using special software. The parameters of hyperfine interaction, such as isomer shift (IS), quadruple splitting (QS), effective internal magnetic field (Heff), line widths (FWHM), and relative weight (G) of the partial components in the spectra were determined.

Catalytic measurements

The catalytic measurements were carried out in an isothermal continuous flow type quartz-glass reactor (6.0 mm inner diameter) at atmospheric pressure. The catalysts were fixed in the reactor between plugs of quartz wool. The following conditions were applied: catalyst fraction 0.63–0.8 mm, catalyst volume 0.3 cm^3, and gas flow mixture of 108 ml/min at $CO:O_2$:He ratio of 4:5:91 vol.%. The reactant gases were supplied through Aalborg electronic mass flow controllers. Analysis of inlet and outlet gas flows was performed online on a HP 5890 gas chromatograph equipped with a thermal conductivity detector and a Carboxen-1000 column. Helium was used as a carrier gas.

RESULTS AND DISCUSSION

Sample XRD patterns are presented in figure 1, which reveal that the starting biogenic material was X-ray amorphous. This is evidence that the biogenic material contained low-crystalline iron oxyhydroxides (probably goethite and lepidocrocite). No characteristic lines of the modifying medium component 0.3% Pd/Al-Si-O in the spectra were registered. This result implies that no significant amount of the modifier was mixed with the biomaterial during cultivation.

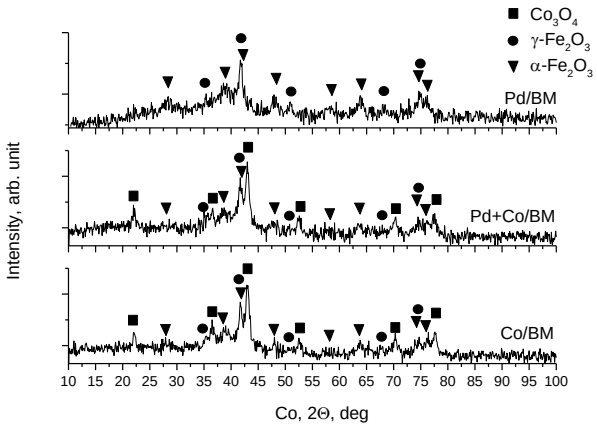

Fig. 1. X-ray diffraction patterns of modified samples thermally treated at 300 °C.

An overall pattern of all measured spectra of the modified biogenic material after calcination at 300 °C indicated chemical phases of low degree of crystallinity, which are characteristic of ultra- and highly dispersed oxide materials. Only iron-containing phases of hematite and maghemite were present in the spectrum of Pd-modified sample, the lines of hematite (α-Fe_2O_3) slightly higher intensity.

XRD patterns for Co_3O_4 (PDF 01-076-1802), γ-Fe_2O_3 (PDF 00-039-1346) and α-Fe_2O_3 (PDF 01-084-0310) are detectable in a Pd+Co/BM sample.

No diffraction peaks for Pd and PdO were visible in the XRD spectrum revealing fine dispersion of the noble metal. The main characteristic lines of the two iron oxide modifications are approximately of the same intensity. The diffraction lines are broad and low intense owing to high dispersion of the iron oxides. The linewidths indicate that the formed materials are ultra- or highly dispersed.

IR results are displayed in figure 2a. A spectrum of Pd/BM sample shows bands characteristic of goethite (3182, 886, 792, 668, 470 cm^{-1}) and lepidocrocite (3182, 1112, 1023, 976, 745 cm^{-1}) as well as surface carbonates (1482 plateau, 1639, 1656, 718 cm^{-1}).

The spectra of Pd+Co/BM, Co/BM, and Mn/BM show bands characteristic of lepidocrocite (3203, 1115, 745, 1021 cm^{-1}), nitrates (825, 1382 cm^{-1}), and surface carbonates (1657, 1640, 1474, 1454, 719 cm^{-1}). Although not all characteristic goethite bands were observed, its presence in the studied systems should be assumed. The materials treated at 300°C were also investigated. The IR spectra are presented in figure 2b. Bands characteristic of Fe-O vibration (under 500 cm^{-1}) prove the presence of iron oxides and Co_3O_4.

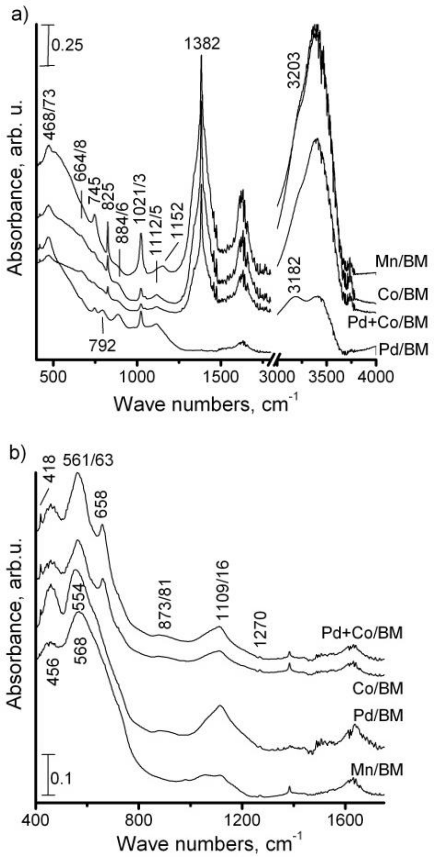

Fig. 2. Infrared spectra of modified samples before (a) and after (b) thermal treatment at 300 °C.

Mössbauer spectra of samples before and after catalytic test are shown in figure 3. Calculated parameters of the spectra are given in Table 1. Results of XRD and Mössbauer spectroscopy studies confirmed the presence of hematite and maghemite in the samples before catalysis. Most spectra except those of Mn/BM and Pd+Co/BM-LNT fit well with a model of two sextets and two doublets. The parameters of both sextets correspond to the two modifications of iron oxide - hematite (α-Fe_2O_3) and maghemite (γ-Fe_2O_3), that of maghemite being more intensive. Both sextets have reduced H_{eff} values of about 10−20 T, which indicated that the particles were highly dispersed. Doublet components in the Mössbauer spectra are indicative of nanosized highly dispersed particles, which demonstrate superparamagnetic behaviour. Polymorph phases ratio of iron oxides before heating to those obtained after heating at 300 °C can be related to thermal decomposition dynamics of the various iron hydroxides.

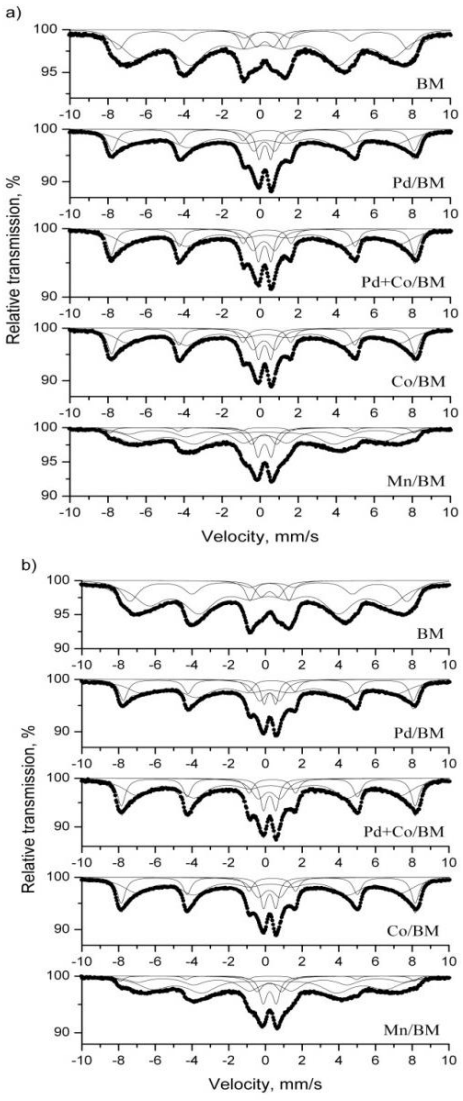

Fig. 3. Room temperature Mössbauer spectra of modified samples thermally treated at 300 °C (a) and after catalytic test (b).

Table 1. Mössbauer parameters of modified samples thermally treated at 300 °C and after CO oxidation reaction

Sample	Components	IS, mm/s	QS, mm/s	H_{eff}, T	FWHM, mm/s	G, %
BM	Sx1 – α-Fe_2O_3	0.37	-0.10	47.3	0.90	18
TS300	Sx2 – γ-Fe_2O_3	0.33	0.00	41.8	1.98	70
	Db1 – SPM	0.36	0.90	-	0.73	6
	Db2 – SPM	0.32	2.13	-	0.56	6
Pd/BM	Sx1 – α-Fe_2O_3	0.36	-0.11	49.4	0.60	22
TS300	Sx2 – γ-Fe_2O_3	0.33	0.03	43.3	2.00	58
	Db1 – SPM	0.34	0.61	-	0.40	9
	Db2 – SPM	0.32	1.10	-	0.76	11
Pd+Co/BM	Sx1 – α-Fe_2O_3	0.36	-0.11	49.6	0.52	25
TS300	Sx2 – γ-Fe_2O_3	0.33	0.00	44.7	1.71	51
	Db1 – SPM	0.33	0.66	-	0.41	11
	Db2 – SPM	0.30	1.15	-	0.80	13
Pd+Co/BM	Sx1 – α-Fe_2O_3	0.47	-0.11	52.3	0.39	33
TS300, LNT	Sx2 – γ-Fe_2O_3	0.41	0.03	49.7	0.90	61
	Db1 – SPM	0.42	0.84	-	0.75	7
Co/BM	Sx1 – α-Fe_2O_3	0.36	-0.10	49.6	0.54	26
TS300	Sx2 – γ-Fe_2O_3	0.33	0.01	44.6	1.67	51
	Db1 – SPM	0.33	0.66	-	0.42	10
	Db2 – SPM	0.30	1.15	-	0.79	13
Mn/BM	Sx1 – α-Fe_2O_3	0.33	-0.11	49.8	0.40	5
TS300	Sx2 – $MnFe_2O_4$	0.38	0.00	44.8	1.39	31
	Sx3 – $MnFe_2O_4$	0.31	0.00	39.3	2.00	45
	Db1 – SPM	0.33	0.70	-	0.46	10
	Db2 – SPM	0.32	1.32	-	0.69	9
BM	Sx1 – α-Fe_2O_3	0.37	-0.10	47.0	1.07	22
TS300, after CO oxidation	Sx2 – γ-Fe_2O_3	0.31	0.00	40.8	2.00	66
	Db1 – SPM	0.34	0.95	-	0.75	6
	Db2 – SPM	0.33	2.12	-	0.59	6
Pd/BM	Sx1 – α-Fe_2O_3	0.36	0.10	49.2	0.56	21
TS300, after CO oxidation	Sx2 – γ-Fe_2O_3	0.34	0.00	43.1	2.00	59
	Db1 – SPM	0.33	0.63	-	0.40	8
	Db2 – SPM	0.33	1.07	-	0.79	12
Pd+Co/BM	Sx1 – α-Fe_2O_3	0.36	-0.11	49.8	0.52	24
TS300, after CO oxidation	Sx2 – γ-Fe_2O_3	0.33	0.01	45.0	1.76	53
	Db1 – SPM	0.33	0.67	-	0.43	10
	Db2 – SPM	0.30	1.18	-	0.89	13
Co/BM	Sx1 – α-Fe_2O_3	0.36	-0.10	49.6	0.54	26
TS300, after CO oxidation	Sx2 – γ-Fe_2O_3	0.33	0.01	44.6	1.67	51
	Db1 – SPM	0.33	0.66	-	0.42	10
	Db2 – SPM	0.30	1.15	-	0.79	13
Mn/BM	Sx1 – α-Fe_2O_3	0.33	-0.11	49.8	0.40	5
TS300, after CO oxidation	Sx2 – $MnFe_2O_4$	0.38	0.00	45.0	1.41	30
	Sx3 – $MnFe_2O_4$	0.31	0.00	39.4	2.00	47
	Db1 – SPM	0.35	0.71	-	0.48	10
	Db2 – SPM	0.32	1.33	-	0.73	8

IS - isomer shift, QS - quadrupole splitting, H_{eff} - effective internal magnetic field, FWHM - line widths, G - relative weight of the partial components in the spectra, LNT- spectra measured at liquid nitrogen temperature

Mössbauer spectrum recorded at the temperature of liquid nitrogen (LNT) showed a decrease of doublet part, which is typical of iron oxide particles of sizes below 4–10 nm (figure 4).

The spectrum of Mn-modified sample preheated at 300 °C differs from the spectra of other samples by lower content of iron phase, which is hematite rhombohedral polymorph (α-Fe_2O_3). In the synthesis of Mn-modified sample, a ferrite $MnFe_2O_4$ phase was formed. It is presented in the spectrum by two sextet components with zero value of the quadruple split, indicating that the ferrite $MnFe_2O_4$ phase has a cubic symmetry. The two components in the spectra correspond to two types of differently coordinated iron ions, tetrahedral and octahedral, and are characteristic of inverse type spinel structure of the fer-

rites. Ferrite phase lines are broad and asymmetrical and the values of the internal magnetic field are reduced. This is due to a size dependent magnetic effect of the particles, which is explained by the presence of finely dispersed structure of the Mn-modified biogenic material.

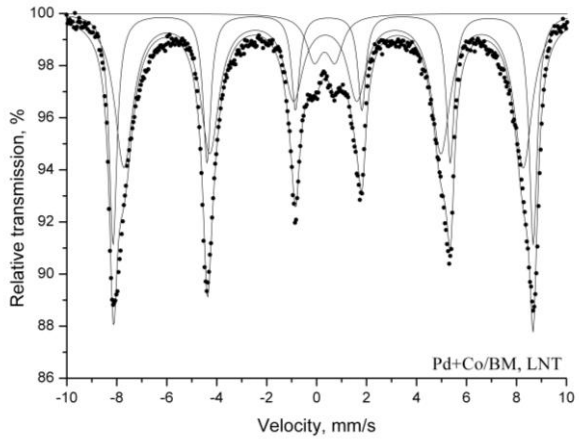

Fig. 4. Liquid nitrogen temperature Mössbauer spectrum of Pd+Co/BM sample thermally treated at 300 °C.

The spectra of all samples measured before and after catalysis are of the same type and matched by the values of calculated superfine parameters. The relative ratio of sextets to doublets was preserved, which indicated that no recrystallization and agglomeration processes occurred at the temperature of catalytic tests.

Temperature dependences of the CO oxidation over unmodified and modified biogenic catalysts are shown in figure 5. Doping with palladium, cobalt, or manganese increased the catalytic activity. The order of activity was Mn/BM > Pd+Co/BM > Co/BM > Pd/BM > BM. As is seen, unmodified biogenic material is active in the studied reaction. The reaction started at about 200 °C and a maximum of 70% conversion was reached at 275 °C. According to literature data, iron oxide materials have been found to be good/proper candidates as cheap and efficient catalysts, especially in environmental processes [36, 37]. As was shown above, the maghemite (γ-Fe_2O_3 70%) is a predominant iron oxide in the initial biogenic material. According to some authors [38] γ-Fe_2O_3 has exhibited a low activity at temperatures lower than 300 °C. Addition of Pd resulted in displacement of the conversion curve to a lower temperature indicating a better catalytic activity. Liu *et al*. [39] claim that the promoting effect of iron oxide in the case of Pd-FeO_x catalysts is related to the ability of the iron oxide species, located in close proximity to the palladium, to provide adsorption sites for oxygen that can subsequently react with CO molecules adsorbed on adjacent Pd sites. Thus, we can conclude that because of the high dispersion of Pd and close interaction between Pd and Fe_2O_3 in Pd/BM sample, more surface oxygen species is provided to the palladium, thus improving its catalytic activity. Modification of Pd/BM sample with cobalt caused a further increase in activity. This is not surprising because unsupported cobalt oxide is a very active species in the field of air pollution control of CO [40,41]. It is known that cobalt catalysts are active for CO oxidation at low temperatures (−70 °C) if pre-oxidised before activity measurement [42, 43].

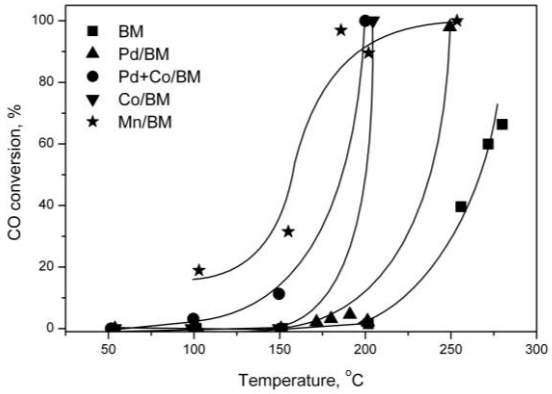

Fig. 5. Conversion vs. temperature in the reaction of CO oxidation.

Mn-modified BM sample manifested the highest catalytic activity. A synergistic effect could be proposed between iron and manganese oxide components. As was shown by Mössbauer spectroscopy a ferrite $MnFe_2O_4$ phase was formed. Formation of solid solutions or $Fe_xMn_yO_4$ spinels has been proposed by Kedesdy and Tauber [44]. It has also been observed that transition metals such as manganese in the spinel lattice can strongly modify the redox properties of the ferrites and therefore activity. To obtain adequate explanation of the synergistic effect further in-depth study of this system is necessary.

CONCLUSIONS

Starting biogenic material is an X-ray amorphous mixture of goethite and lepidocrocite iron oxyhydroxides having ultradispersed nanosized particles with adsorbed surface nitrate and carbonate groups. Modification of the biogenic material with Pd, Pd+Co, and Co and subsequent calcination led to the formation of Co_3O_4, γ-Fe_2O_3, and α-Fe_2O_3. A highly dispersed $MnFe_2O_4$ ferrite phase was formed in Mn-modified sample. It has a cubic symmetry, spinel structure, and inverse ion distribution. It was proved by Mössbauer spectroscopy that the iron oxides and $MnFe_2O_4$ ferrite were nanosized highly dispersed entities. Metal ions oxidation state, phase composition, and dispersion of the test samples did not

change during catalytic tests. Catalytic measurements showed that all prepared samples were active in the reaction of CO oxidation and the catalytic properties depended on dopant type. A synergistic effect was proposed between iron and manganese oxide components.

Acknowledgements: *This work is financially supported by National Science Fund through project DFNI T02-17/12.12.2014. The authors are grateful to Prof. V. Groudeva and R. Angelova from Faculty of Biology of St. Kliment Ohridski University of Sofia for providing iron-containing biogenic material.*

REFERENCES

1. D. Ellis, Microbiology of the Iron-depositing Bacteria, Wexford College Press, Palm Springs, CA, 2003.
2. A. Kappler, K. L. Straub, *Rev. Miner. Geochem*., **59**, 85 (2005).
3. Z. Cherkezova-Zheleva, D. Paneva, M. Shopska, R. Ilieva, M. Iliev, D. Kovacheva, G. Kadinov, *Hyperfine Interact.*, **239**, 6 (2018).
4. M. Shopska, D. Paneva, Z. Cherkezova-Zheleva, G. Kadinov, I. Mitov, V. Grudeva, *Nanoscience & Nanotechnology*, **14**, 21 (2014).
5. D. Emerson, E. J. Fleming and J. M. McBeth, *Annu. Rev. Microbiol*., **64**, 561 (2010).
6. H. L. Ehrlich, D. K. Newman, Geomicrobiology, CRC Press, Boca Raton, 2009.
7. C. Chan, S. Fakra, D. Edwards, D. Emerson, J. Banfield, *Geochim. Cosmochim. Acta*, **73**, 3807 (2009).
8. F. G. Ferris, R. O. Hallberg, B. Lyven, K. Pedersen, *Appl. Geochem*., **15**, 1035 (2000).
9. K. Benzerara, T. Yooh, T. Tyliszczak, B. Constantz, A. Spormann, G. Brown, Jr., *Geobiology*, **2**, 249 (2004).
10. T. Ema, Y. Miyazaki, I. Kozuki, T. Sakai, H. Hashimoto, J. Takada, *Green Chem*., **13**, 3187 (2011).
11. X. Wang, M. Zhu, S. Lan, M. Ginder-Vogel, F. Liu, X. Feng, *Chem. Geol*., **415**, 37 (2015).
12. Z. Cherkezova-Zheleva, M. Shopska, D. Paneva, D. Kovacheva, G. Kadinov, I. Mitov, *Hyperfine Interact*., **237**, 56 (2016).
13. T. Sakai, Y. Miyazaki, A. Murakami, N. Sakamoto, T. Ema, H. Hashimoto, M. Furutani, M. Nakanishi, T. Fujiia, J. Takada, *Org. Biomol. Chem*., **8**, 336 (2010).
14. P. C. Francisco, T. Sato, T. Otake, T. Kasama, *Am. Mineral*., **101**, 2057 (2016).
15. J. A. Rentz, Phosphorus Removal Potential Using Biogenic Iron Oxides, WERF Research Report Series, vol. 10, IWA Publishing, London, 2010.
16. D. Pragnesh, C. Lakhan, *J. Nanotechnol*., Article ID 398569 (2014).
17. M. Shopska, D. Paneva, G. Kadinov, S. Todorova, M. Fabian, I. Yordanova, Z. Cherkezova-Zheleva, I. Mitov, *Reac. Kinet. Mech. Catal*., **118**, 179 (2016).
18. M. Shopska, D. Paneva, G. Kadinov, Z. Cherkezova-Zheleva, I. Mitov, M. Iliev, *Appl. Biochem. Biotechnol*., **181**, 867 (2017).
19. M. Shopska, Z. Cherkezova-Zheleva, D. Paneva, M. Iliev, G. Kadinov, I. Mitov, V. Groudeva, *Cent. Eur. J. Chem*., **11**, 215 (2013).
20. K. B. Narayanan, N. Sakthivel, *Adv. Colloid Interface Sci*., **156**, 1 (2010).
21. H. Hashimoto, S. Yokoyama, H. Asaoka, Y. Kusano, Y. Ikeda, M. Seno, J. Takada, T. Fujii, M. Nakanishi, R. Murakami, *J. Magnet. Magnet. Mater*., **310**, 2405 (2007).
22. D. Emerson, H. Lin, L. Agulto, L. Lin, *Bioscience*, **58**, 925 (2008).
23. J. S. J. Hargreaves, A. I. Alharthi, *J. Chem. Technol. Biotechnol*., **91**, 296 (2016).
24. B. Kazprzyk-Hordern, M. Ziolek, J. Nawrocik, *Appl. Catal. B*., **46**, 639 (2003).
25. T. Shahwan, S. Abu Sirriah, M. Nairat, E. Boyaci, A. E. Eroglu, T. B. Scott, K. R. Hallam, *Chem. Eng. J*., **172**, 258 (2011).
26. B. Kumar, K. Smita, L. Cumbal, A. Debut, *J. Saudi. Chem. Soc*., **18**, 364 (2014).
27. G. E. Hoag, J. B. Collins, J. L. Holcomb, J. R. Hoag, M. N. Nadagouda, R. S. Varma, *J. Mater. Chem*., **19**, 8671 (2009).
28. H. Jung, H. Park, J. Kim, J-H Lee, H-G Hur, N. V. Myung, H. Choi, *Environ. Sci. Technol*., **41**, 4741 (2007).
29. M. G. Shopska, G. B. Kadinov, J. Briancin, I. D. Yordanova, H. G. Kolev, M. Fabian, *Bulg. Chem. Commun*., **47** (Special Issue C), 79 (2015).
30. M. Shopska, S. Todorova, I. Yordanova, S. Mondal, G. Kadinov, *Bulg. Chem. Commun*., **47** (Special Issue C), 73 (2015).
31. S. Y. Lee, M. H. Baik, H-R Cho, E. C. Jung, J. T. Jeong, J. W. Choi, Y. B. Lee, Y. J. Lee, *J. Radioanal. Nucl. Chem*., **296**, 1311 (2013).
32. A. Alharthi, R. A. Blackley, T. H. Flowers, J. S. J. Hergreaves, I. D. Pulford, J. Wigzell, W. Zhou, *J. Chem. Technol. Biotechnol*., **89**, 1317 (2014).
33. K. Mandai, T. Korenaga, T. Ema, T. Sakai, M. Furutani, H. Hashimoto, J. Takada, *Tetrahedron Lett.*, **53**, 329 (2012).
34. M. Harshiny, C. N. Iswarya, M. Matheswaran, *Powder Technol*., **286**, 744 (2015).
35. T. Ema, Y. Miyazaki, T. Taniguchi, J. Takada, *Green Chem*., **15**, 2485 (2013).
36. M. Mohapatra, S. Anand, *Int. J. Eng. Sci. Technol*., **2**, 127 (2010).
37. S. C. Kwon, M. Fan, T. D. Wheelock, B. Saha, *Sep. Purif. Technol*., **58**, 40 (2007).
38. L. C. A. Oliveira, J. D. Fabris, R. R. V. A. Rios, W. N. Mussel, R. M. Lago, *Appl. Catal. A: Gen*., **259**, 253 (2004).
39. L. Liu, F. Zhou, L. Wang, X. Qi, F. Shi, Y. Deng, *J. Catal*., **274**, 1 (2010).
40. Y. J. Mergler, J. Hoebink, B. E. Nieuwenhuys, *J. Catal*., **167**, 305 (1997).
41. J. Jansson, *J. Catal*., **194**, 55 (2000).
42. P. Thormählen, M. Skoglundh, E. Fridell, B. Andersson, *J. Catal*., **188**, 300 (1999).

43. D. A. H. Cunningham, T. Kobayashi, N. Kamijo, M. Haruta, *Catal. Lett.*, **25**, 257 (1994).
44. H. H. Kedesdy, A. Tauber, *J. Americ. Ceram. Soc.*, **39**, 425 (1956).

МОДИФИЦИРАНЕ И ОХАРАКТЕРИЗИРАНЕ НА ЖЕЛЯЗОСЪДЪРЖАЩИ БИОГЕННИ МАТЕРИАЛИ КАТО КАТАЛИЗАТОРИ ЗА РЕАКЦИЯТА НА ОКИСЛЕНИЕ НА CO

Т. М. Петрова*, Д. Г. Панева, С. Ж. Тодорова, З. П. Черкезова-Желева, Д. Г. Филкова, М. Г. Шопска, Н. И. Велинов, Б. Н. Кунев, Г. Б. Кадинов, Ив. Г. Митов

Институт по катализ, Българска академия на науките, ул. „Акад. Г. Бончев“, бл. 11, 1113 София, България

Постъпила на 12 февруари 2018 г.; Преработена на 14 март 2018 г.

(Резюме)

Настоящото изследване е насочено към получаване на модифицирани желязо-съдържащи биогенни материали и тяхното изпитване като катализатори в реакцията на окисление на CO. Модифицирането е осъществено чрез импрегниране на биогенен материал, получен в хранителна среда Lieske. Импрегнирането е извършено с използване на разтвори на паладиев хлорид, кобалтов нитрат и манганов нитрат. Пробите са охарактеризирани с рентгенова дифракция (XRD), инфрачервена и Мьосбауерова спектроскопия. Резултатите от XRD показват, че изходният биогенен материал е рентгеноаморфен, но въпреки това не се изключва наличието на смес от нискокристални железни оксихидроксиди гьотит и лепидокрокит. Нагряване на Pd- и Co-модифицирани материали води до образуване на фази от Co_3O_4, γ-Fe_2O_3 и α-Fe_2O_3. В термично третираните проби, инфрачервените спектри потвърждават пълно трансформиране на оксихидроксидите до оксиди. Мьосбауерови спектри на проби обработени при 300 °C показват, че образуваните материали имат ниска степен на кристалност, която е специфична характеристика за наноразмерни високо дисперсни оксидни материали. Дублетни компоненти в Мьосбауеровите спектри са показателни за наличието на наноразмерни високо-дисперсни частици демонстриращи суперпарамагнитно поведение. При синтеза на образец модифициран с манган се формира феритна $MnFe_2O_4$ фаза. Мьосбауеров спектър, регистриран при температурата на течен азот, показва намаляване на дублетната част, което е типично за железни оксидни частици с размер под 4–10 nm. Всички изследвани образци показват активност в реакцията на окисление на CO, като най-високо активен е катализаторът модифициран с манган. Анализ на Мьосбауеровите спектри на пробите след каталитични тестове не показва промени във фазовия състав и дисперсността.